



UNIVERSITAT DE
BARCELONA

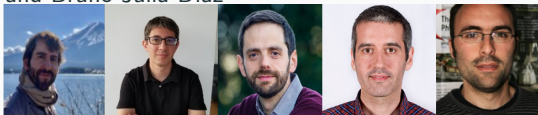


Barcelona
Supercomputing
Center
Centro Nacional de Supercomputación

Simulating nuclei in digital quantum computers

Antonio Márquez Romero - a.marquez.romero@fqa.ub.edu

— In collaboration with Axel Pérez Obiol, Javier Menéndez, Arnau Ríos, Artur García Sáez and Bruno Juliá Díaz



arXiv:2302.03641

Nuclear and particle physics on a quantum computer: where do we stand now?

ECT* Trento, Italy

5th June 2023

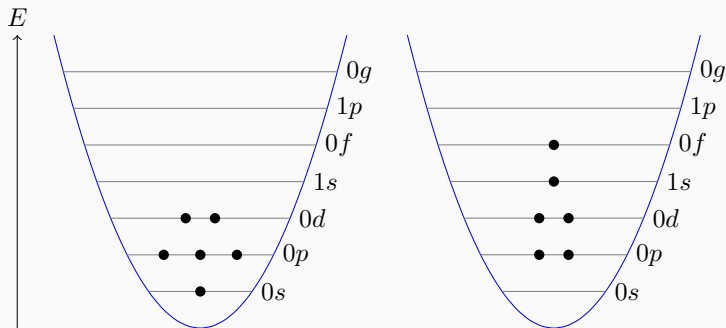
Motivation

Motivation

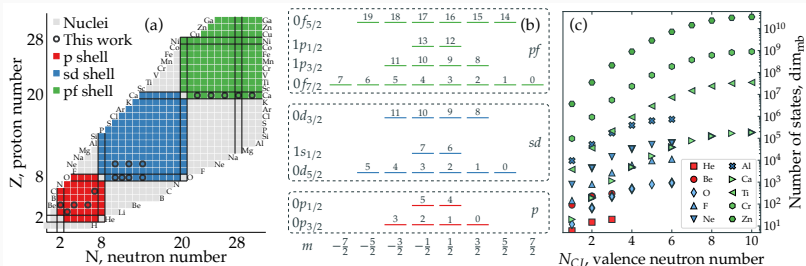
- The shell model is a Nobel prize-winning theory for the description of nuclear structure but faces the “dimensionality problem”.

Motivation

- The shell model is a Nobel prize-winning theory for the description of nuclear structure but faces the “dimensionality problem”.
- Calculations involve diagonalization of Hamiltonian matrices in a many-body basis that scales combinatorially with the valence-space dimension and number of nucleons.



Motivation



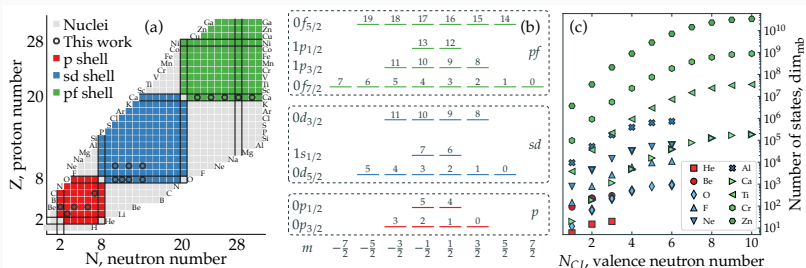
Quantum algorithms may facilitate the solution to physical problems that scale exponentially in a classical computer:

$$|Q\rangle = a_0|0\rangle + a_1|1\rangle$$

$$|Q_1Q_2\rangle = a_{00}|00\rangle + a_{01}|01\rangle + a_{10}|10\rangle + a_{11}|11\rangle$$

$$|Q_1Q_2Q_3\rangle = a_{000}|000\rangle + a_{001}|001\rangle + a_{010}|010\rangle + a_{100}|100\rangle \\ + a_{011}|011\rangle + a_{101}|101\rangle + a_{110}|110\rangle + a_{111}|111\rangle$$

Motivation



Quantum algorithms may facilitate the solution to physical problems that scale exponentially in a classical computer:

$$|Q\rangle = a_0|0\rangle + a_1|1\rangle$$

$$|Q_1Q_2\rangle = a_{00}|00\rangle + a_{01}|01\rangle + a_{10}|10\rangle + a_{11}|11\rangle$$

$$|Q_1Q_2Q_3\rangle = a_{000}|000\rangle + a_{001}|001\rangle + a_{010}|010\rangle + a_{100}|100\rangle \\ + a_{011}|011\rangle + a_{101}|101\rangle + a_{110}|110\rangle + a_{111}|111\rangle$$

Implementation in quantum devices comes with other challenges.

Specifics of the project

- Variational quantum eigensolvers (VQE) are a promising tool for the description of nuclear structure with quantum circuits.

¹J Tilly, et al., The variational quantum eigensolver: a review of methods and best practices. Phys. Reports 986, 1–128 (2022)

Specifics of the project

- Variational quantum eigensolvers (VQE) are a promising tool for the description of nuclear structure with quantum circuits.
- In its implementation, different strategies are to be pursued for the following challenges¹:

¹J Tilly, et al., The variational quantum eigensolver: a review of methods and best practices. Phys. Reports 986, 1–128 (2022)

Specifics of the project

- Variational quantum eigensolvers (VQE) are a promising tool for the description of nuclear structure with quantum circuits.
- In its implementation, different strategies are to be pursued for the following challenges¹:
 - State preparation

¹J Tilly, et al., The variational quantum eigensolver: a review of methods and best practices. Phys. Reports 986, 1–128 (2022)

Specifics of the project

- Variational quantum eigensolvers (VQE) are a promising tool for the description of nuclear structure with quantum circuits.
- In its implementation, different strategies are to be pursued for the following challenges¹:
 - State preparation
 - Fermionic operator encoding

¹J Tilly, et al., The variational quantum eigensolver: a review of methods and best practices. Phys. Reports 986, 1–128 (2022)

Specifics of the project

- Variational quantum eigensolvers (VQE) are a promising tool for the description of nuclear structure with quantum circuits.
- In its implementation, different strategies are to be pursued for the following challenges¹:
 - State preparation
 - Fermionic operator encoding
 - Iterative optimization and convergence

¹J Tilly, et al., The variational quantum eigensolver: a review of methods and best practices. Phys. Reports 986, 1–128 (2022)

Specifics of the project

- Variational quantum eigensolvers (VQE) are a promising tool for the description of nuclear structure with quantum circuits.
- In its implementation, different strategies are to be pursued for the following challenges¹:
 - State preparation
 - Fermionic operator encoding
 - Iterative optimization and convergence
 - Measurement

¹J Tilly, et al., The variational quantum eigensolver: a review of methods and best practices. Phys. Reports 986, 1–128 (2022)

Specifics of the project

- Variational quantum eigensolvers (VQE) are a promising tool for the description of nuclear structure with quantum circuits.
- In its implementation, different strategies are to be pursued for the following challenges¹:
 - State preparation
 - Fermionic operator encoding
 - Iterative optimization and convergence
 - Measurement
 - Error mitigation

¹J Tilly, et al., The variational quantum eigensolver: a review of methods and best practices. Phys. Reports 986, 1–128 (2022)

Specifics of the project

- Variational quantum eigensolvers (VQE) are a promising tool for the description of nuclear structure with quantum circuits.
- In its implementation, different strategies are to be pursued for the following challenges¹:
 - State preparation
 - Fermionic operator encoding
 - Iterative optimization and convergence
 - Measurement
 - Error mitigation
- We expect resources in a quantum computer do not scale exponentially, as in a classical supercomputer

¹J Tilly, et al., The variational quantum eigensolver: a review of methods and best practices. Phys. Reports 986, 1–128 (2022)

Classical simulation

Adaptive variational quantum eigensolver (ADAPT-VQE)⁴

Starting ingredients: a reference state $|\Psi_{\text{ref}}\rangle$ and a pool of operators

$$\hat{A}_m : a_i^\dagger a_j, a_i^\dagger a_j^\dagger a_l a_k \dots$$

Adaptive variational quantum eigensolver (ADAPT-VQE)⁴

Starting ingredients: a reference state $|\Psi_{\text{ref}}\rangle$ and a pool of operators

$$\hat{A}_m : a_i^+ a_j, a_i^+ a_j^+ a_l a_k \dots$$

Algorithm:

$$|\Psi_0\rangle = |\Psi_{\text{ref}}\rangle$$

$$|\Psi_1\rangle = e^{i\theta_1 \hat{A}_1} |\Psi_0\rangle$$

$$|\Psi_2\rangle = e^{i\theta_2 \hat{A}_2} |\Psi_1\rangle = \underbrace{e^{i\theta_2 \hat{A}_2}}_{\text{layer 2}} \underbrace{e^{i\theta_1 \hat{A}_1}}_{\text{layer 1}} |\Psi_0\rangle$$

⋮

$$|\Psi_n\rangle = \underbrace{e^{i\theta_n \hat{A}_n} \dots e^{i\theta_1 \hat{A}_1}}_{\text{layers}} |\Psi_0\rangle$$

Adaptive variational quantum eigensolver (ADAPT-VQE)⁴

Starting ingredients: a reference state $|\Psi_{\text{ref}}\rangle$ and a pool of operators

$$\hat{A}_m : a_i^+ a_j, a_i^+ a_j^+ a_l a_k \dots$$

Algorithm:

$$|\Psi_0\rangle = |\Psi_{\text{ref}}\rangle$$

$$|\Psi_1\rangle = e^{i\theta_1 \hat{A}_1} |\Psi_0\rangle$$

$$|\Psi_2\rangle = e^{i\theta_2 \hat{A}_2} |\Psi_1\rangle = \underbrace{e^{i\theta_2 \hat{A}_2}}_{\text{layer 2}} \underbrace{e^{i\theta_1 \hat{A}_1}}_{\text{layer 1}} |\Psi_0\rangle$$

⋮

$$|\Psi_n\rangle = \underbrace{e^{i\theta_n \hat{A}_n} \dots e^{i\theta_1 \hat{A}_1}}_{\text{layers}} |\Psi_0\rangle$$

Operators \hat{A}_m selected according to the largest gradient

$$\left. \frac{\partial E^{(k)}}{\partial \theta_m} \right|_{\theta_m=0} = i \langle \Psi_k | [\hat{H}, \hat{A}_m] | \Psi_k \rangle$$

Adaptive variational quantum eigensolver (ADAPT-VQE)⁴

Starting ingredients: a reference state $|\Psi_{\text{ref}}\rangle$ and a pool of operators

$$\hat{A}_m : a_i^+ a_j, a_i^+ a_j^+ a_l a_k \dots$$

Algorithm:

$$|\Psi_0\rangle = |\Psi_{\text{ref}}\rangle$$

$$|\Psi_1\rangle = e^{i\theta_1 \hat{A}_1} |\Psi_0\rangle$$

$$|\Psi_2\rangle = e^{i\theta_2 \hat{A}_2} |\Psi_1\rangle = \underbrace{e^{i\theta_2 \hat{A}_2}}_{\text{layer 2}} \underbrace{e^{i\theta_1 \hat{A}_1}}_{\text{layer 1}} |\Psi_0\rangle$$

⋮

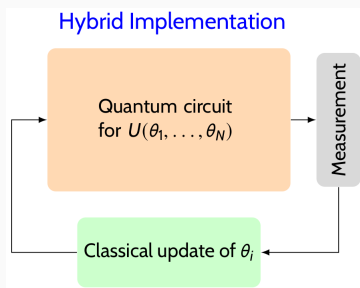
$$|\Psi_n\rangle = \underbrace{e^{i\theta_n \hat{A}_n} \dots e^{i\theta_1 \hat{A}_1}}_{\text{layers}} |\Psi_0\rangle$$

Operators \hat{A}_m selected according to the largest gradient

$$\left. \frac{\partial E^{(k)}}{\partial \theta_m} \right|_{\theta_m=0} = i \langle \Psi_k | [\hat{H}, \hat{A}_m] | \Psi_k \rangle$$

Parameters θ_m obtained minimizing the energy surface at every iteration.

⁴ Grimsley, H.R., Economou, S.E., Barnes, E. et al. Nat Commun 10, 3007 (2019)



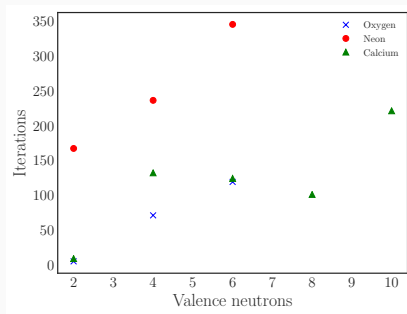
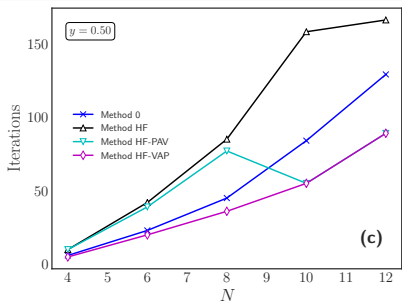
Courtesy of Jon Engel

Good scaling!

Previous work with ADAPT-VQE in the Lipkin and shell-model²:

Lipkin model of N particles with interaction strength y

sd - and pf -shell phenomenological interactions



²AM Romero, J. Engel, Ho Lun Tang, and Sophia E. Economou. PRC 105, 064317

A comparison between VQEs

What's the impact of Trotterization? That is

$$e^{\hat{A}+\hat{B}} = \lim_{n \rightarrow \infty} (e^{\hat{A}/n} e^{\hat{B}/n})^n.$$

³I. Stetcu et al. Phys. Rev. C 105, 064308, O. Kiss et al, Phys. Rev. C 106, 034325

A comparison between VQEs

What's the impact of Trotterization? That is

$$e^{\hat{A}+\hat{B}} = \lim_{n \rightarrow \infty} (e^{\hat{A}/n} e^{\hat{B}/n})^n.$$

Main difference between the Unitary Coupled Cluster (UCC)³ approach and ADAPT

$$|\Psi\rangle_{\text{UCC}} = e^{i \sum_k \theta_k \hat{A}_k} |\Psi_0\rangle,$$
$$|\Psi\rangle_{\text{ADAPT}} = \prod_k e^{i \theta_k \hat{A}_k} |\Psi_0\rangle.$$

	UCC		ADAPT	
	parameters	ε_E	parameters	ε_E
⁸ Be	112	10^{-2}	48	10^{-7}
²² O	35	10^{-2}	20	10^{-2}
⁶ Li	9	10^{-7}	9	10^{-7}

³I. Stetcu et al. Phys. Rev. C 105, 064308, O. Kiss et al, Phys. Rev. C 106, 034325

Quantum implementation

Implementation in quantum devices: fermionic mapping

Jordan-Wigner mapping is used for convenience:

$$a_i^\dagger = \left(\prod_{k=0}^{i-1} Z_k \right) \sigma_i^-, \quad a_i = \left(\prod_{k=0}^{i-1} Z_k \right) \sigma_i^+,$$

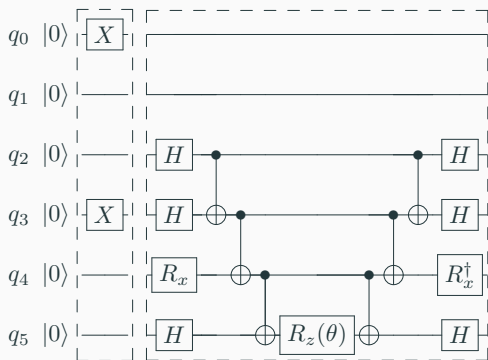
with $\sigma_k^\pm = \frac{1}{2}(X_k \pm iY_k)$.

Jordan-Wigner transformation of relevant operators

	Fermion Operators	Qubit Operators
n_p	$a_p^\dagger a_p$	$\frac{1}{2}(1 - Z_p)$
h_{pqrs}	$a_p^\dagger a_q^\dagger a_r a_s$ $+ a_r^\dagger a_s^\dagger a_p a_q$	$\frac{1}{8} P_{rs}^{pq} (- X_p X_q X_r X_s + X_p X_q Y_r Y_s$ $- X_p Y_q X_r Y_s - X_p Y_q Y_r X_s$ $- Y_p Y_q Y_r Y_s + Y_p Y_q X_r X_s$ $- Y_p X_q Y_r X_s - Y_p X_q X_r Y_s)$
T_{rs}^{pq}	$i(a_p^\dagger a_q^\dagger a_r a_s$ $- a_r^\dagger a_s^\dagger a_p a_q)$	$\frac{1}{8} P_{rs}^{pq} (- X_p Y_q Y_r Y_s - Y_p X_q Y_r Y_s$ $+ Y_p Y_q X_r Y_s + Y_p Y_q Y_r X_s$ $+ Y_p X_q X_r X_s + X_p Y_q X_r X_s$ $- X_p X_q Y_r X_s - X_p X_q X_r Y_s)$

$$P_{rs}^{pq} \equiv \left(\prod_{m=p+1, m \notin [r,s]}^{q-1} Z_m \right) \left(\prod_{n=r+1, n \notin [p,q]}^{s-1} Z_n \right)$$

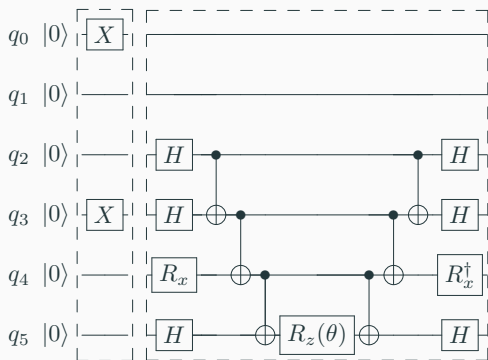
Implementation in quantum devices: CNOT staircase



with $R_x = e^{-i\frac{\pi}{2}X}$ and $R_z(\theta) = e^{-i\frac{\theta}{2}Z}$. This circuit builds the wavefunction

$$|\Psi\rangle^{6\text{Be}} = e^{-i\frac{\theta}{2}X_2X_3Y_4Z_5}|\Psi_{0,3}\rangle^{6\text{Be}}.$$

Implementation in quantum devices: CNOT staircase



with $R_x = e^{-i\frac{\pi}{2}X}$ and $R_z(\theta) = e^{-i\frac{\theta}{2}Z}$. This circuit builds the wavefunction

$$|\Psi\rangle^{6\text{Be}} = e^{-i\frac{\theta}{2}X_2X_3Y_4Z_5}|\Psi_{0,3}\rangle^{6\text{Be}}.$$

CNOTs drive the feasibility of the circuit.

Measurement of the energy

$$H = \sum_i \varepsilon_i a_i^\dagger a_i + \frac{1}{4} \sum_{ijkl} \bar{v}_{ijkl} a_i^\dagger a_j^\dagger a_l a_k$$

Measurement of the energy

$$H = \sum_i \varepsilon_i a_i^\dagger a_i + \frac{1}{4} \sum_{ijkl} \bar{v}_{ijkl} a_i^\dagger a_j^\dagger a_l a_k$$

We disentangle them in

- Single-particle terms: $n_i = a_i^\dagger a_i$
- Local terms: $h_{ijij} = -2n_i n_j$
- Single-hopping terms: $h_{ijkj} = a_i^\dagger a_i (a_j^\dagger a_k + a_k^\dagger a_j)$
- Double-hopping terms: $h_{ijkl} = a_i^\dagger a_j^\dagger a_l a_k + a_l^\dagger a_k^\dagger a_i a_j$

Measurement of the energy

$$H = \sum_i \varepsilon_i a_i^\dagger a_i + \frac{1}{4} \sum_{ijkl} \bar{v}_{ijkl} a_i^\dagger a_j^\dagger a_l a_k$$

We disentangle them in

- Single-particle terms: $n_i = a_i^\dagger a_i$
- Local terms: $h_{ijij} = -2n_i n_j$
- Single-hopping terms: $h_{ijki} = a_i^\dagger a_i (a_j^\dagger a_k + a_k^\dagger a_j)$
- Double-hopping terms: $h_{ijkl} = a_i^\dagger a_j^\dagger a_l a_k + a_l^\dagger a_k^\dagger a_i a_j$

After the JW mapping

- $\langle \Psi_k | n_i | \Psi_k \rangle = \frac{1}{2} \langle \Psi_k | 1 - Z_i | \Psi_k \rangle = p_1^{(i)}$
- $\langle \Psi_k | h_{ijij} | \Psi_k \rangle = -2p_{11}^{(ij)}$
- $\langle \Psi_k | h_{ijik} | \Psi_k \rangle = p_{101}^{(ijk)} - p_{110}^{(ijk)}$
- $\langle \Psi_k | h_{ijkl} | \Psi_k \rangle = p_{1100}^{(ijkl)} - p_{0011}^{(ijkl)}$

Measurement of the energy

$$H = \sum_i \varepsilon_i a_i^\dagger a_i + \frac{1}{4} \sum_{ijkl} \bar{v}_{ijkl} a_i^\dagger a_j^\dagger a_l a_k$$

We disentangle them in

- Single-particle terms: $n_i = a_i^\dagger a_i$
- Local terms: $h_{ijij} = -2n_i n_j$
- Single-hopping terms: $h_{ijki} = a_i^\dagger a_i (a_j^\dagger a_k + a_k^\dagger a_j)$
- Double-hopping terms: $h_{ijkl} = a_i^\dagger a_j^\dagger a_l a_k + a_l^\dagger a_k^\dagger a_i a_j$

After the JW mapping

- $\langle \Psi_k | n_i | \Psi_k \rangle = \frac{1}{2} \langle \Psi_k | 1 - Z_i | \Psi_k \rangle = p_1^{(i)}$
- $\langle \Psi_k | h_{ijij} | \Psi_k \rangle = -2p_{11}^{(ij)}$
- $\langle \Psi_k | h_{ijik} | \Psi_k \rangle = p_{101}^{(ijk)} - p_{110}^{(ijk)}$
- $\langle \Psi_k | h_{ijkl} | \Psi_k \rangle = p_{1100}^{(ijkl)} - p_{0011}^{(ijkl)}$

How many circuits are needed to measure the energy?

Basis-change circuits

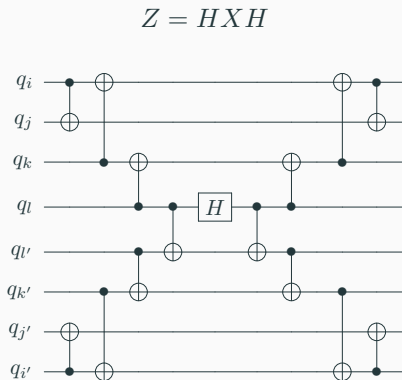


Figure 2: Quantum circuit to implement the change of basis to diagonalize $\langle \Psi_k | h_{ijkl} | \Psi_k \rangle$.

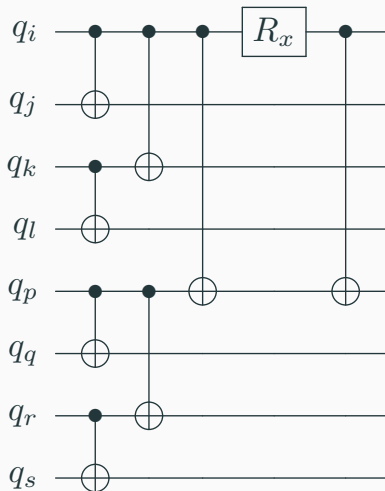


Figure 3: Quantum circuit to implement the change of basis to diagonalize $\langle \Psi_k | h_{ijkl} T_{rs}^{pq} | \Psi_k \rangle$

Number of circuits for measurement

shell	N_{qb}	N_h	N_{hh}	Total
p	6	2	10 (9)	13 (12)
	12	4	109 (44)	114 (49)
sd	12	8	203 (86)	212 (95)
	24	16	1389 (518)	1406 (535)
pf	20	20	1507 (570)	1528 (591)
	40	40	10572 (3459)	10613 (3500)

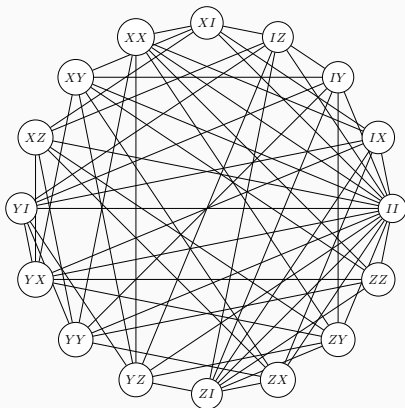
Table 1: Number of different circuits needed to measure the expectation value of the Hamiltonian. N_h and N_{hh} are the number of single- and double-hopping terms in the Hamiltonian. The values in parenthesis correspond to the minimum number of groups containing h_{ijkl} terms found such that all operators in the group commute with each other and can be measured with the same circuit. In the last column, the total number of circuits corresponding to $N_h + N_{hh} + 1$, accounting also for the single circuit needed to measure $\langle n_i \rangle$ and $\langle h_{ijij} \rangle$.

Measurement: minimum clique problem

Dimension of two-body excitation operators increases quartically with space dimensionality and can not be measured simultaneously. We need to find the minimum partition group of commuting operators

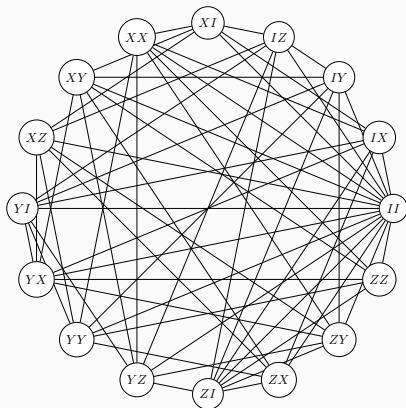
Measurement: minimum clique problem

Dimension of two-body excitation operators increases quartically with space dimensionality and can not be measured simultaneously. We need to find the minimum partition group of commuting operators



Measurement: minimum clique problem

Dimension of two-body excitation operators increases quartically with space dimensionality and can not be measured simultaneously. We need to find the minimum partition group of commuting operators



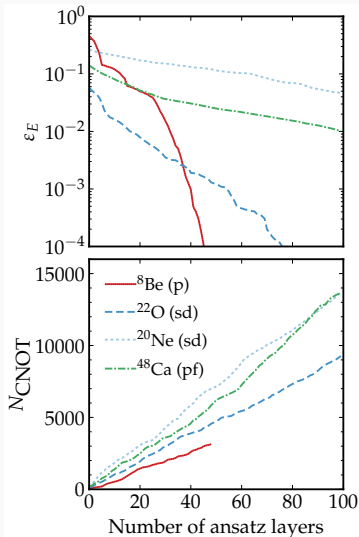
NP-hard problem! We used a greedy algorithm for approximate solutions

Results

Polynomial scaling of the quantum resources

shell	N_{qb}	N_{SD}	nucleus	N_l	ϵ_E	N_C
<i>p</i>	6	5	${}^6\text{Be}$	2	10^{-8}	42
	12	10	${}^6\text{Li}$	9	10^{-7}	92
		53	${}^8\text{Be}$	48	10^{-7}	68
		51	${}^{10}\text{Be}$	48	10^{-7}	62
		21	${}^{13}\text{C}$	19	10^{-7}	77
<i>sd</i>	12	14	${}^{18}\text{O}$	5	10^{-6}	99
		37	${}^{19}\text{O}$	32	10^{-6}	85
		81	${}^{20}\text{O}$	70	10^{-6}	98
		142	${}^{22}\text{O}$	117	10^{-6}	93
	24	640	${}^{20}\text{Ne}$	167	2×10^{-2}	137
		4206	${}^{22}\text{Ne}$	236	2×10^{-2}	137
		7562	${}^{24}\text{Ne}$	345	2×10^{-2}	138
<i>pf</i>	20	30	${}^{42}\text{Ca}$	9	10^{-8}	116
		565	${}^{44}\text{Ca}$	132	10^{-2}	153
		3952	${}^{46}\text{Ca}$	124	10^{-2}	139
		12022	${}^{48}\text{Ca}$	101	10^{-2}	137
		17276	${}^{50}\text{Ca}$	221	10^{-2}	130

Table 2: N_{qb} : number of qubits, N_{SD} : number of many-body basis states, N_l : number of layers (parameters), ϵ_E : relative error in energy and N_C : number of CNOTs per layer



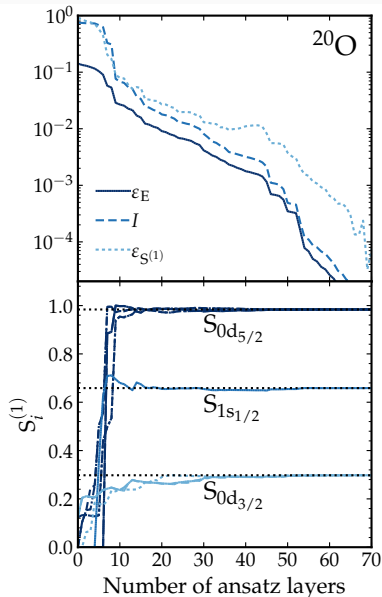
Quantum information tools for nuclear structure

- We can study nuclear structure properties with quantum information tools.
- Infidelity: $I = 1 - |\langle \Psi_{gs} | \Psi_k \rangle|^2$
- Single-particle entanglement entropies⁵:

$$S_i^{(1)} = -n_i \log_2(n_i) - (1 - n_i) \log_2(1 - n_i)$$

⁵Robin, Savage & Pillet. PRC 103(3), 034325 (2021)

$0d_{3/2}$	<u>11</u>	<u>10</u>	<u>9</u>	<u>8</u>		
$1s_{1/2}$		<u>7</u>	<u>6</u>			
$0d_{5/2}$	<u>5</u>	<u>4</u>	<u>3</u>	<u>2</u>	<u>1</u>	<u>0</u>
m	$-\frac{5}{2}$	$-\frac{3}{2}$	$-\frac{1}{2}$	$\frac{1}{2}$	$\frac{3}{2}$	$\frac{5}{2}$



Quantum information tools for nuclear structure

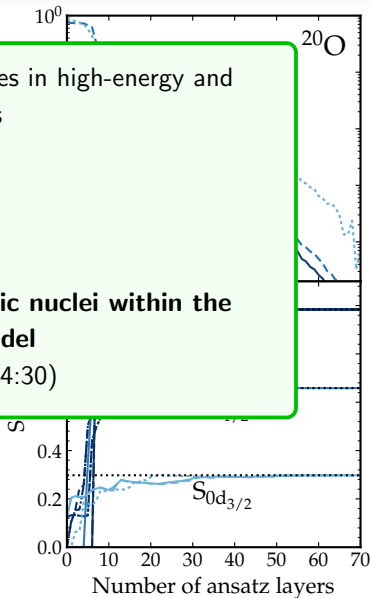
- We can study nuclear structure properties with quantum

Thursday: entanglement perspectives in high-energy and nuclear physics

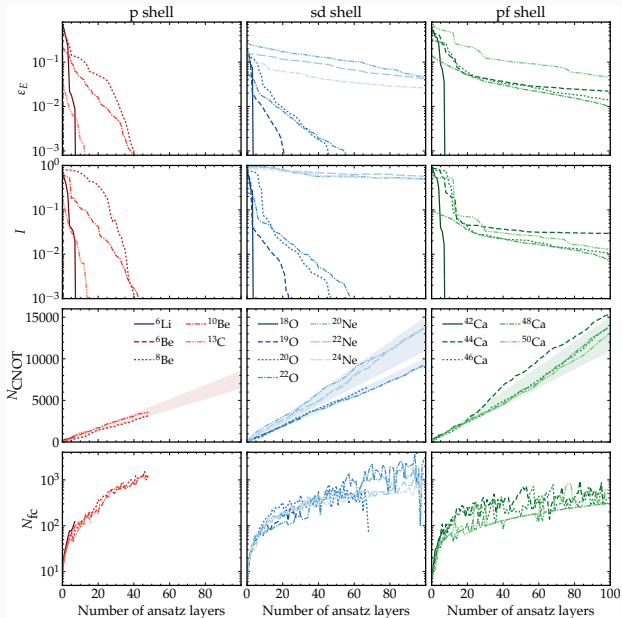
Entanglement entropies in atomic nuclei within the nuclear shell model

Axel Pérez Obiol (14:30)

$0d_{3/2}$	<u>11</u>	<u>10</u>	<u>9</u>	<u>8</u>		
$1s_{1/2}$		<u>7</u>	<u>6</u>			
$0d_{5/2}$	<u>5</u>	<u>4</u>	<u>3</u>	<u>2</u>	<u>1</u>	<u>0</u>
m	$-\frac{5}{2}$	$-\frac{3}{2}$	$-\frac{1}{2}$	$\frac{1}{2}$	$\frac{3}{2}$	$\frac{5}{2}$



Summary of all simulated nuclei in this work



Model circuit

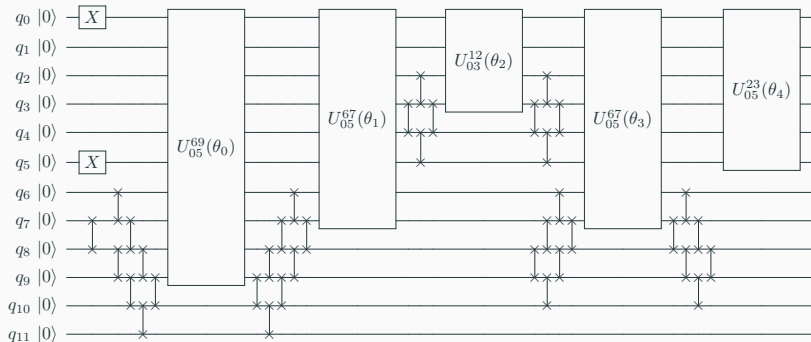


Figure 4: Quantum circuit to prepare the exact ground-state of ^{18}O . FSWAPS are used to change basis so that exponentials of pool operators operate on adjacent qubits. Multiqubit gates in the boxes are defined as $U_{ij}^{kl}(\theta) \equiv e^{i\theta T_{ij}^{kl}}$ and $\theta_0 = -0.157263$, $\theta_1 = -0.437238$, $\theta_2 = 0.604663$, $\theta_3 = 0.214431$, $\theta_4 = -0.785469$.

$$|\Psi_{18\text{O}}\rangle = e^{i\theta_4 T_{23}^{05}} e^{i\theta_3 T_{910}^{05}} e^{i\theta_2 T_{14}^{05}} e^{i\theta_1 T_{67}^{05}} e^{i\theta_0 T_{811}^{05}} X_0 X_5 |0\rangle^{\otimes 12}.$$

Conclusions

Conclusions

- Promising results were obtained using ADAPT-VQE applied with phenomenological shell-model interactions in the classical and quantum simulation of the algorithm.
- The quantum implementation of VQE carries challenges of its own that hopefully are easier to solve than the exponential scaling. It is of particular interest the application of quantum information tools to strongly-correlated systems such as atomic nuclei.
- We developed a baseline code with the quantum implementation of the nuclear shell-model to explore and study these upcoming challenges⁴.

⁴UB+BSC collaboration, arXiv:2302.03641

Corresponding author: a.marquez.romero@fqa.ub.edu

Conclusions

- Promising results were obtained using ADAPT-VQE applied with phenomenological shell-model interactions in the classical and quantum simulation of the algorithm.
- The quantum implementation of VQE carries challenges of its own that hopefully are easier to solve than the exponential scaling. It is of particular interest the application of quantum information tools to strongly-correlated systems such as atomic nuclei.
- We developed a baseline code with the quantum implementation of the nuclear shell-model to explore and study these upcoming challenges⁴.

Grazie mille!

⁴UB+BSC collaboration, arXiv:2302.03641

Corresponding author: a.marquez.romero@fqa.ub.edu

Extra slides

Fermionic mapping: example and potential alternative

The general Hamiltonian:

$$H = \sum_i \varepsilon_i a_i^\dagger a_i + \frac{1}{4} \sum_{ijkl} \bar{v}_{ijkl} a_i^\dagger a_j^\dagger a_l a_k, \quad (1)$$

under a JW mapping, the corresponding matrix representation will have $2^{\dim} \times 2^{\dim}$ elements.

⁵RMN Pesce, PD Stevenson: H2ZIXY, arXiv:2111.00627

Fermionic mapping: example and potential alternative

The general Hamiltonian:

$$H = \sum_i \varepsilon_i a_i^\dagger a_i + \frac{1}{4} \sum_{ijkl} \bar{v}_{ijkl} a_i^\dagger a_j^\dagger a_l a_k, \quad (1)$$

under a JW mapping, the corresponding matrix representation will have $2^{\dim} \times 2^{\dim}$ elements.

Example:

Take the case of ${}^6\text{Li}$ in the M -scheme: ground-state is formed with 10 $M = 0$ states, but with JW the Hamiltonian matrix is $2^{12} \times 2^{12}$!

⁵RMN Pesce, PD Stevenson: H2ZIXY, arXiv:2111.00627

Fermionic mapping: example and potential alternative

The general Hamiltonian:

$$H = \sum_i \varepsilon_i a_i^\dagger a_i + \frac{1}{4} \sum_{ijkl} \bar{v}_{ijkl} a_i^\dagger a_j^\dagger a_l a_k, \quad (1)$$

under a JW mapping, the corresponding matrix representation will have $2^{\dim} \times 2^{\dim}$ elements.

Example:

Take the case of ${}^6\text{Li}$ in the M -scheme: ground-state is formed with 10 $M = 0$ states, but with JW the Hamiltonian matrix is $2^{12} \times 2^{12}$!

Compact encoding of the Hamiltonian⁵:

$$H = 0.598IIII - 0.088IIIX + \dots - 0.037ZZZX - 0.059ZZZZ. \quad (2)$$

Only 4 qubits are needed! But what do projections 0 and 1 represent?

⁵RMN Pesce, PD Stevenson: H2ZIXY, arXiv:2111.00627

Why ADAPT and not Unitary Coupled Clusters approach?

$$|\Psi(\boldsymbol{\theta})\rangle = e^{\hat{T}(\boldsymbol{\theta})}|0\rangle \longrightarrow E_{\text{UCC}} = \min_{\boldsymbol{\theta}} \frac{\langle\Psi(\boldsymbol{\theta})|H|\Psi(\boldsymbol{\theta})\rangle}{\langle\Psi(\boldsymbol{\theta})|\Psi(\boldsymbol{\theta})\rangle}, \quad (3)$$

⁶I. Stetcu et al. Phys. Rev. C 105, 064308

⁷O. Kiss et al, Phys. Rev. C 106, 034325

Why ADAPT and not Unitary Coupled Clusters approach?

$$|\Psi(\boldsymbol{\theta})\rangle = e^{\hat{T}(\boldsymbol{\theta})}|0\rangle \longrightarrow E_{\text{UCC}} = \min_{\boldsymbol{\theta}} \frac{\langle \Psi(\boldsymbol{\theta}) | H | \Psi(\boldsymbol{\theta}) \rangle}{\langle \Psi(\boldsymbol{\theta}) | \Psi(\boldsymbol{\theta}) \rangle}, \quad (3)$$

- ADAPT requires no Trotter approximation

$$e^{A+B} = \lim_{n \rightarrow \infty} \left(e^{A/n} e^{B/n} \right)^n, \quad (4)$$

Good results are obtained with only one Trotter step⁶. Although symmetries can be broken in the wavefunction and be more crucial in strongly-correlated systems

⁶I. Stetcu et al. Phys. Rev. C 105, 064308

⁷O. Kiss et al, Phys. Rev. C 106, 034325

Why ADAPT and not Unitary Coupled Clusters approach?

$$|\Psi(\boldsymbol{\theta})\rangle = e^{\hat{T}(\boldsymbol{\theta})}|0\rangle \longrightarrow E_{\text{UCC}} = \min_{\boldsymbol{\theta}} \frac{\langle \Psi(\boldsymbol{\theta}) | H | \Psi(\boldsymbol{\theta}) \rangle}{\langle \Psi(\boldsymbol{\theta}) | \Psi(\boldsymbol{\theta}) \rangle}, \quad (3)$$

- ADAPT requires no Trotter approximation

$$e^{A+B} = \lim_{n \rightarrow \infty} \left(e^{A/n} e^{B/n} \right)^n, \quad (4)$$

Good results are obtained with only one Trotter step⁶. Although symmetries can be broken in the wavefunction and be more crucial in strongly-correlated systems

- ADAPT does not depend on the cluster operator order

⁶I. Stetcu et al. Phys. Rev. C 105, 064308

⁷O. Kiss et al, Phys. Rev. C 106, 034325

Why ADAPT and not Unitary Coupled Clusters approach?

$$|\Psi(\boldsymbol{\theta})\rangle = e^{\hat{T}(\boldsymbol{\theta})}|0\rangle \longrightarrow E_{\text{UCC}} = \min_{\boldsymbol{\theta}} \frac{\langle \Psi(\boldsymbol{\theta}) | H | \Psi(\boldsymbol{\theta}) \rangle}{\langle \Psi(\boldsymbol{\theta}) | \Psi(\boldsymbol{\theta}) \rangle}, \quad (3)$$

- ADAPT requires no Trotter approximation

$$e^{A+B} = \lim_{n \rightarrow \infty} \left(e^{A/n} e^{B/n} \right)^n, \quad (4)$$

Good results are obtained with only one Trotter step⁶. Although symmetries can be broken in the wavefunction and be more crucial in strongly-correlated systems

- ADAPT does not depend on the cluster operator order
- However, it is possible that ADAPT leads to deeper circuits⁷

⁶I. Stetcu et al. Phys. Rev. C 105, 064308

⁷O. Kiss et al, Phys. Rev. C 106, 034325